

Simulating Low Cloud Evolution by Building a Comprehensive Library of Observed Lagrangian Trajectories



Ehsan Erfani¹, Robert Wood², Peter Blossey², Sarah Doherty², Ryan Eastman², Lucas McMichael²

1 Desert Research Institute, Reno, NV, USA
2 University of Washington, Seattle, WA, USA

Correspondence to: Ehsan.Erfani@dri.edu



1. Background

Challenges:

- Significant **uncertainties** exist in regional and global modeling of **marine low clouds** over the eastern subtropical oceans because those models do not resolve many of the **complex physical processes** including aerosol-cloud interactions.
- The evolution of these clouds and their response to aerosols are **sensitive** to ambient **environmental conditions**.

Objectives:

- Creating a **comprehensive library** of Lagrangian observations in order to represent a **full range** of environmental conditions common in marine low cloud regions.
- Developing a methodology to **routinely initialize and force detailed LES with satellite and reanalysis data**, rather than in-situ measurements, which are rare over remote oceans.

2. Methodology

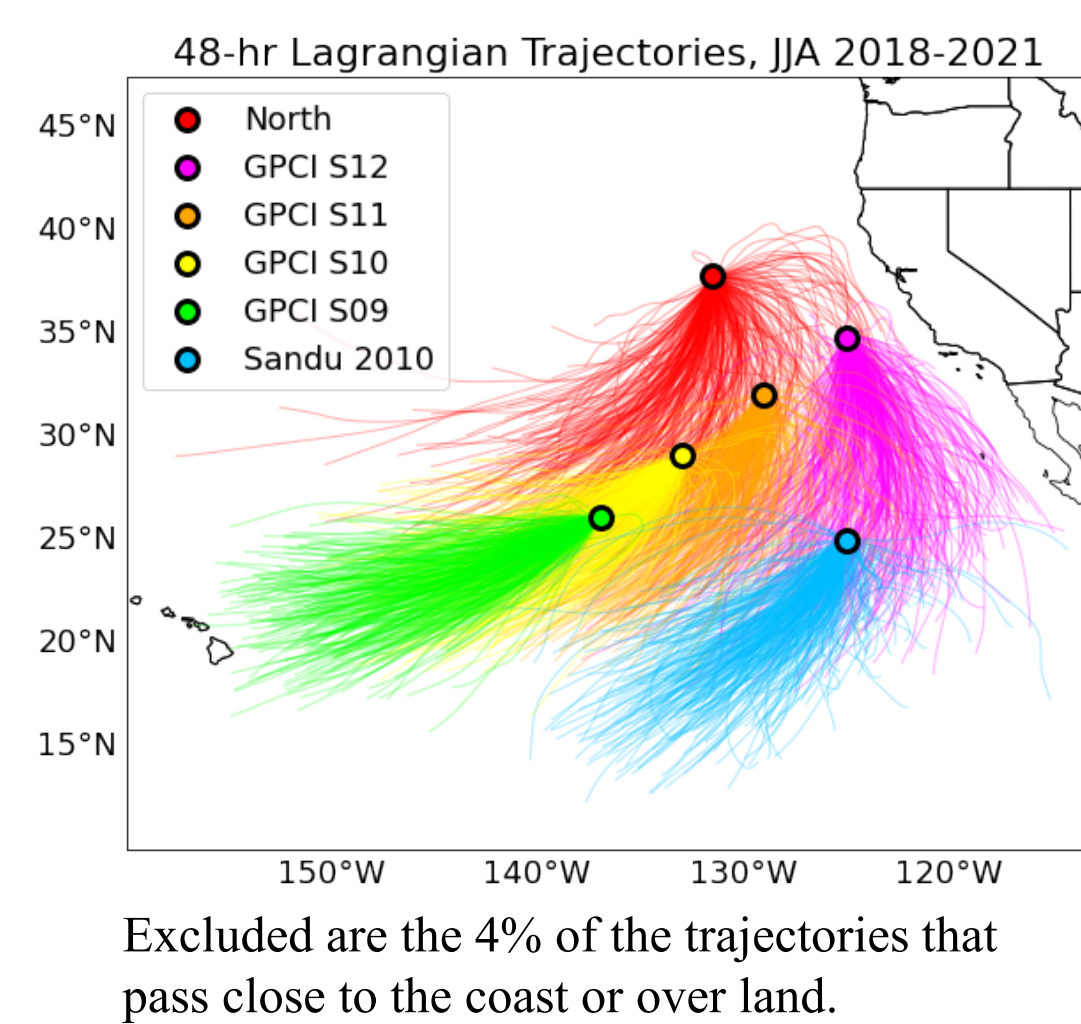
Data

- Cloud-controlling factors (CCFs):** extracted from **ECMWF ERA5 reanalysis data**. sea-surface temperature (SST), Estimated inversion strength (EIS), surface wind speed (WS), free-tropospheric (FT) moisture (q), FT subsidence (ω), mean sea level pressure (P_{MSL}), and inversion height (Z_{inv}).
- Cloud and radiation variables:** extracted from **various satellite observations**. low cloud fraction (CF), liquid water path (LWP), cloud-top height (CTH), precipitation, cloud droplet number concentration (N_d), and effective radius (r_e).
- Aerosol variables:** marine boundary layer (MBL)-averaged accumulation-mode aerosol number concentration ($\langle N_d \rangle$) calculated from NASA MERRA2 masses of aerosol species and their assumed **particle size distributions** (Erfani et al., 2022).

Dataset	ERA5 (meteorology)	MERRA2 (aerosol)	CERES SYN L3 (cloud)	SSM/I V08 L3	AMSR-2 V08 L3	AMSR-2 V08 L3	MODIS
Important Variables	WS, P, T, q, ω , EIS, SST, Z_{inv} , w_e , CF, LWP	N_d	CF, LWP, CTH, N_d , r_e , τ_e , OLR, CRE	LWP	LWP	rain rate	CTH
Reference	Hersbach et al. (2020)	Gelaro et al. (2017)	Doelling et al. (2016)	Wentz et al. (2012)	Kawanishi et al. (2003)	Eastman et al. (2019)	Eastman et al. (2017)
Temporal Resolution	Hourly	3-hourly	Hourly	Two times per day	Two times per day	Two times per day	01:30 LT 13:30 LT
Spatial Resolution	0.25°×0.25°	0.5°×0.625°	1°×1°	0.25°×0.25°	0.25°×0.25°	0.25°×0.25°	1°×1°

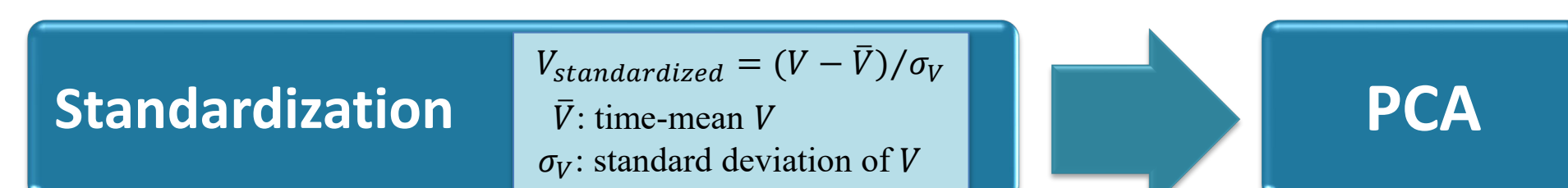
Trajectories

- A few locations in the **stratocumulus deck** region of the Northeast Pacific during JJA 2018–2021 were selected to **fill out a phase space** of CCFs and cloud variables.
- UW trajectory codes were employed to generate **2208 Lagrangian isobaric (950 hPa) forward trajectories** for 82 hours, **incorporating** meteorological, cloud, and aerosol variables obtained from reanalysis and satellite data.



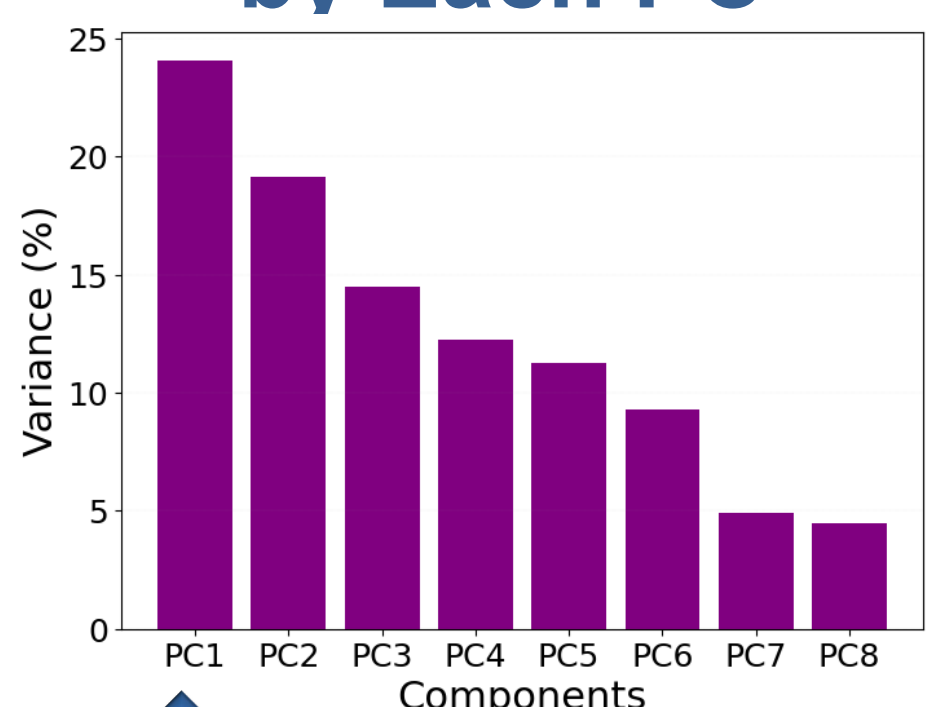
PCA

- Principal Component Analysis (PCA)** was applied to **reduce the dimensionality** and to select a reduced set of **principal components (PCs)**.
- We included all 6 initial locations and all days in JJA 2018–2021, **excluding trajectories with clouds that have a large ice content** (a total of **1663 trajectories** were used).



3. PCA and Phase Space

Percentage of Variance Explained by Each PC



Relationships Between PCs and Variables

PCA inputs: 8 variables (differences between beginning and end of trajectory, and along-trajectory means for CCFs: WS, q , ω , and EIS)

2 CCFs (SST and P_{MSL}) and cloud variables are excluded from PCA.

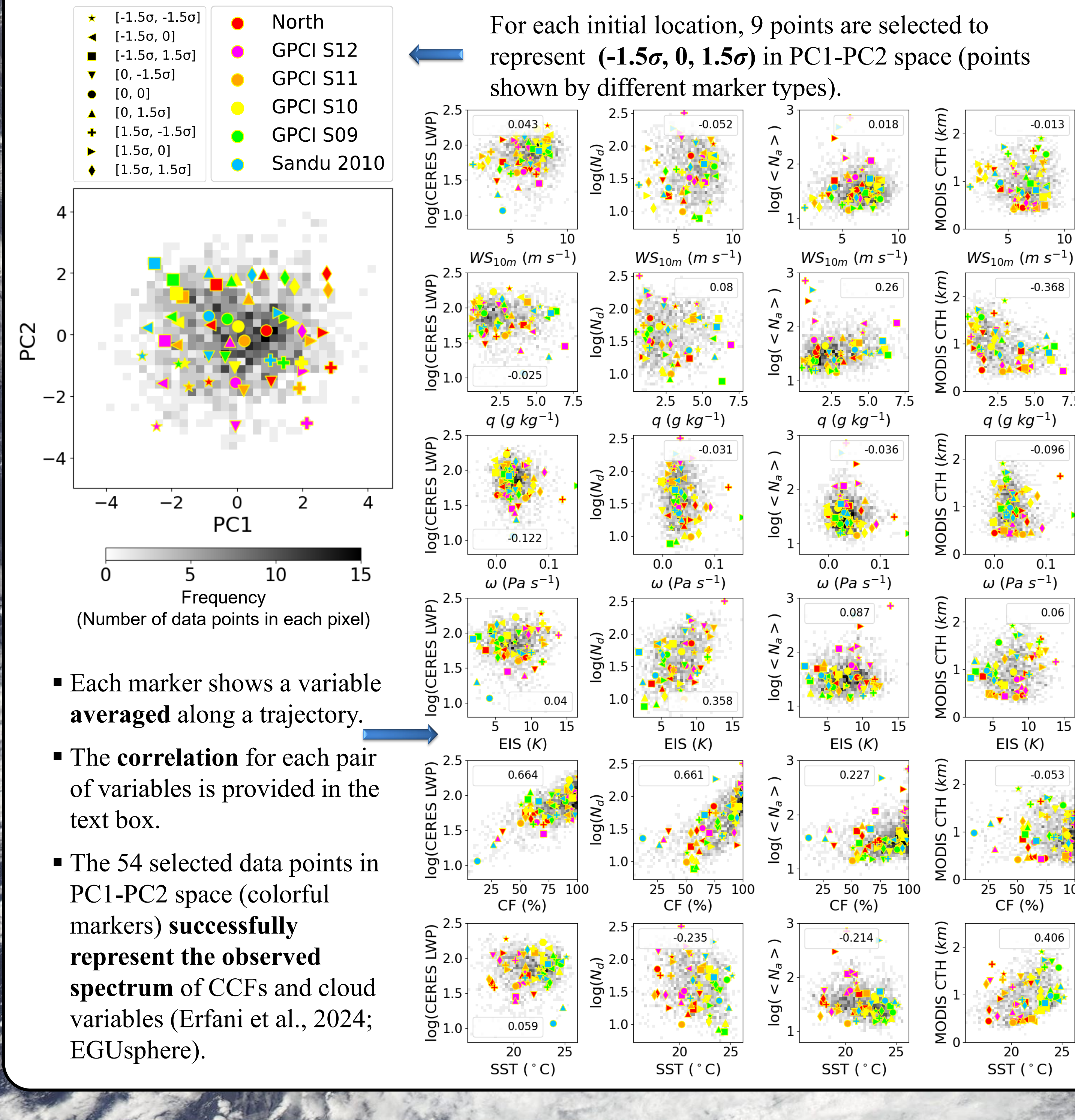
PC	ΔWS_{10m} ($m s^{-1}$)	Δq ($g kg^{-1}$)	$\Delta \omega$ ($Pa s^{-1}$)	ΔEIS (K)	WS_{10m} ($m s^{-1}$)	q ($g kg^{-1}$)	ω ($Pa s^{-1}$)	EIS (K)	CF (%)	SST ($^{\circ}C$)	P_{MSL} (hPa)	log(CERES LWP)	log(N_d)	log($\langle N_d \rangle$)	MODIS CTH (km)	log(Precip)
PC1	-0.03	-0.38	0.02	0.78	-0.43	-0.72	0.48	0.48	-0.07	-0.47	0.21	-0.04	-0.06	-0.17	0.15	-0.1
PC2	0.6	-0.56	0.23	0.39	-0.15	0.29	0	-0.74	-0.34	0.38	0.12	-0.05	-0.37	-0.19	0.02	0.19

- We conducted **one PCA** based on 8 variables (differences between beginning and end of the trajectory, and along-trajectory means for CCFs: EIS, q , ω , and WS).
- 43%** of the information is compressed into **PC1 and PC2**.

- The **Correlations (R-values)** between PCs and all variables
- ΔEIS** and mean q contribute the most to PC1 and mean EIS and AWS contribute the most to PC2.
- Here, an absolute **R-value of 0.14** or higher is statistically significant since it leads to a p-value smaller than 0.05 for non-directional conditions.

Phase Space

For each initial location, 9 points are selected to represent **(-1.5 σ , 0, 1.5 σ)** in PC1-PC2 space (points shown by different marker types).



- Each marker shows a variable **averaged** along a trajectory.
- The **correlation** for each pair of variables is provided in the text box.
- The 54 selected data points in PC1-PC2 space (colorful markers) **successfully represent the observed spectrum** of CCFs and cloud variables (Erfani et al., 2024; EGU sphere).

4. Large-Eddy Simulations

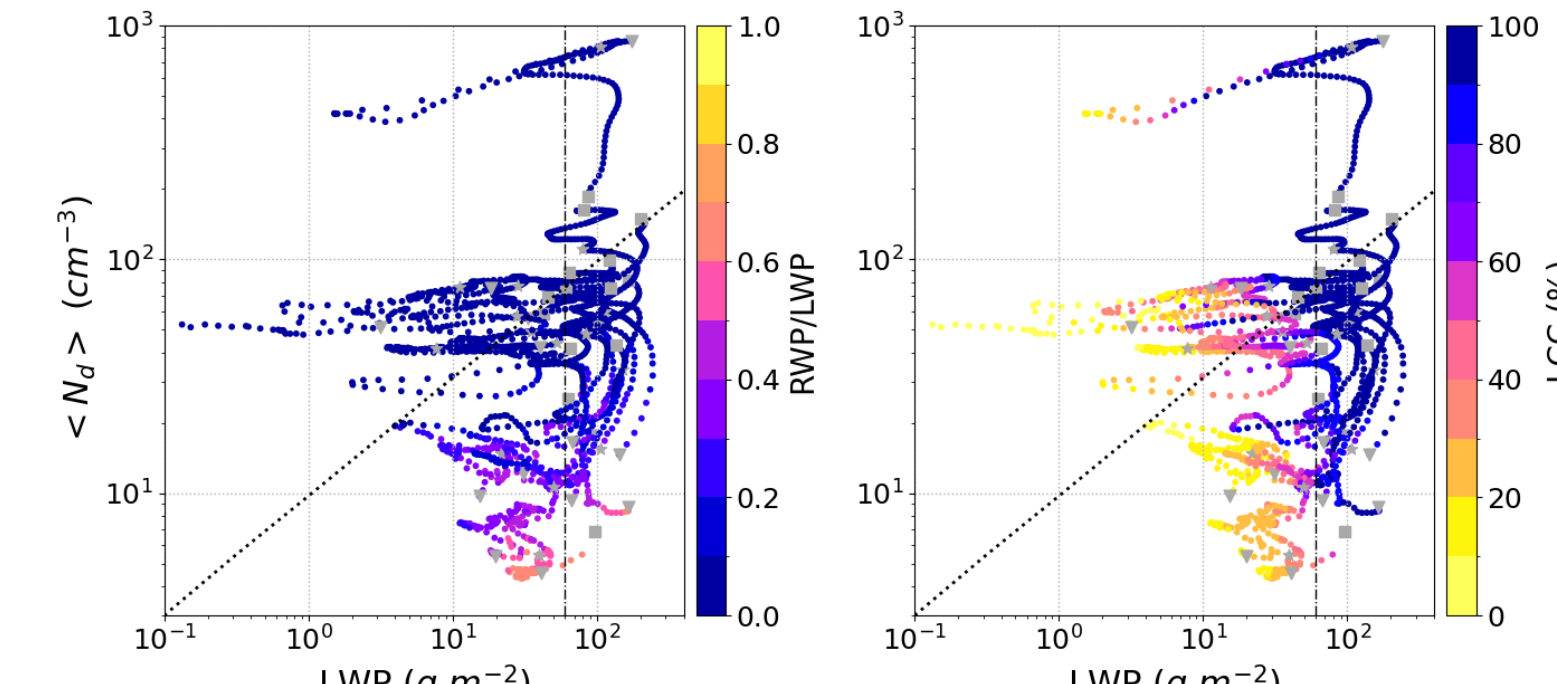
- System for Atmospheric Modeling (SAM)
- Coupled** to Berner aerosol scheme: calculates **MBL aerosol tendencies** due to accretion, autoconversion, interstitial scavenging, surface sources, sedimentation, and entrainment from the FT.
- LES is forced by **meteorological and aerosol variables** compiled along the trajectory.
- Here, such simulations along **15 sample trajectories** are analyzed.

Experiments:

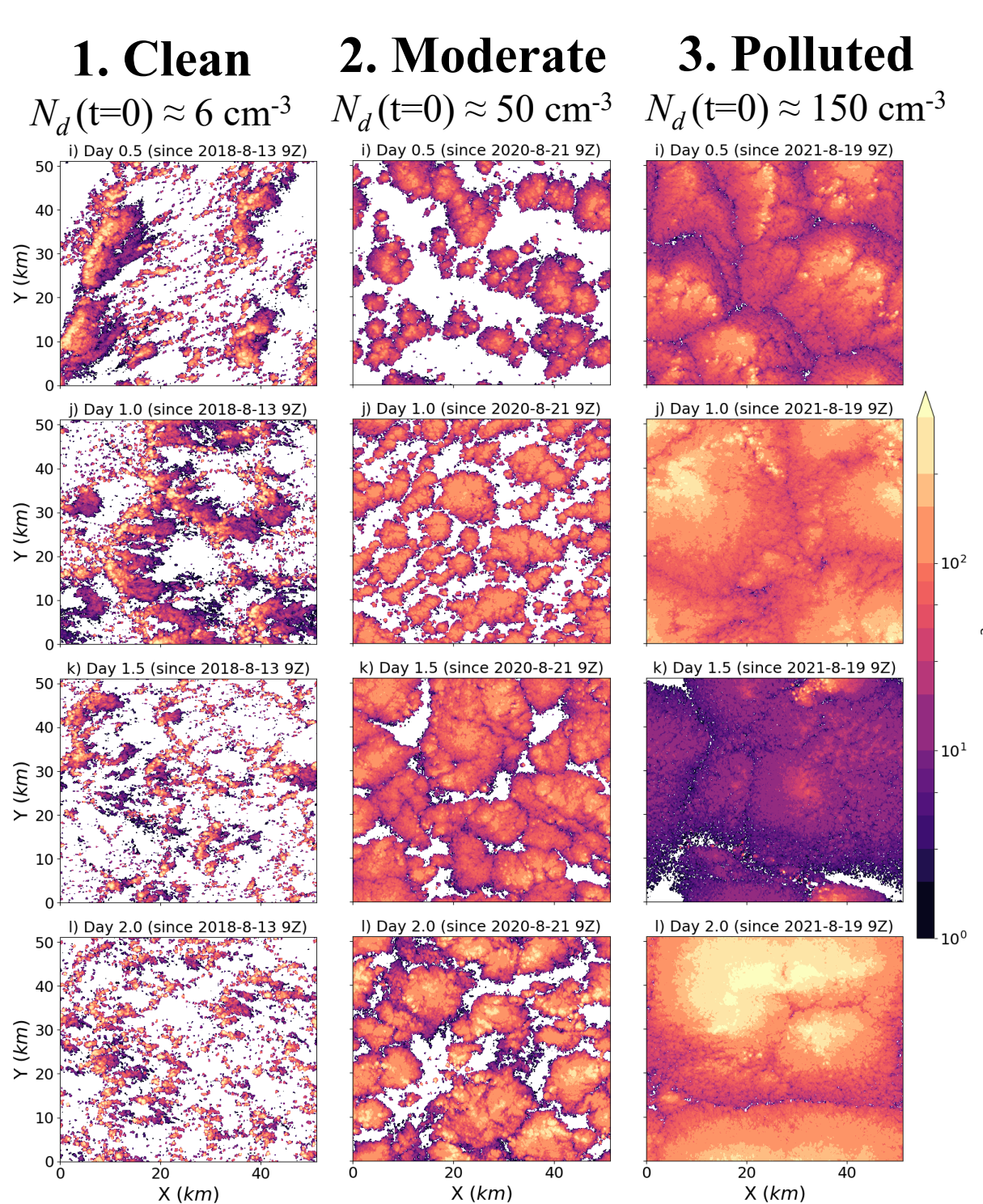
# of cases	Initial MBL N_d	FT N_d	Run Time	Horizontal resolution	Domain size	Vertical level #
15	CERES-corrected MERRA2	MERRA2	48 hrs.	100×100 m	51.2×51.2 km	260

Evolution of 15 Runs in LWP- N_d State Space:

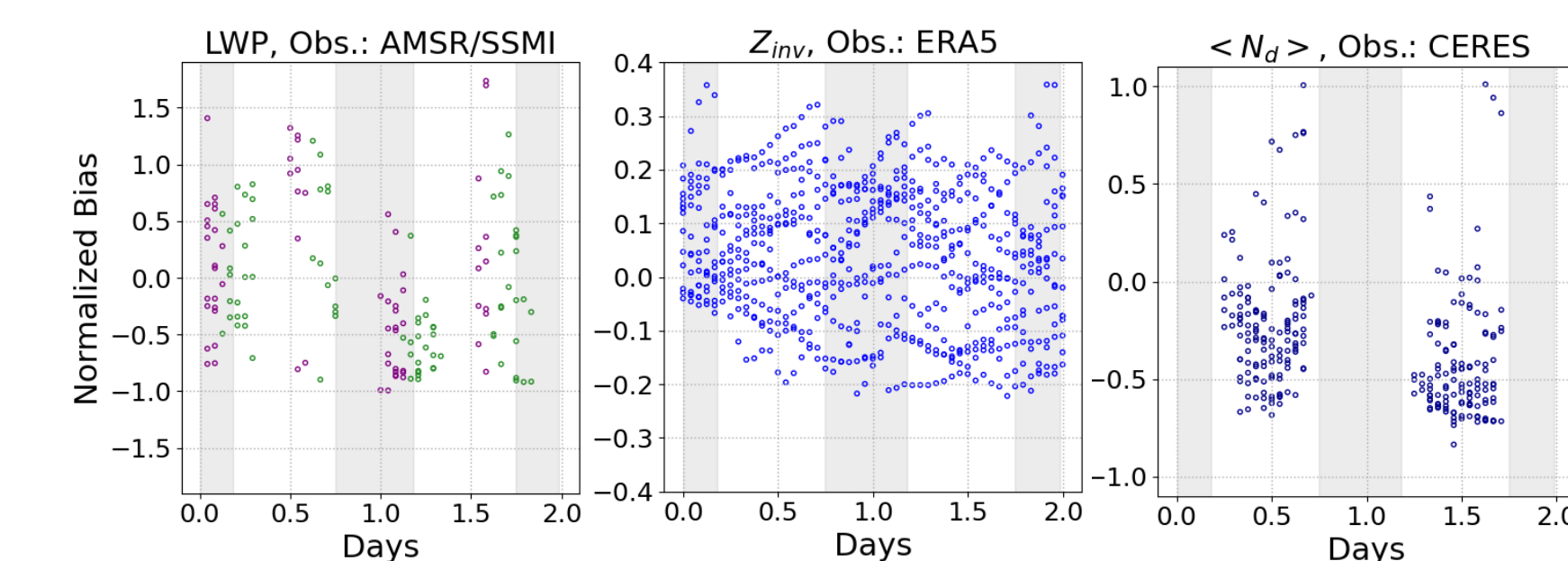
- Theoretically, the **precipitation onset** is quantified by **critical radius** $\approx 12 \mu m$ (Glassmeier et al., 2019). For $r > 12 \mu m$, cases show either initially-low N_d or a rapid decrease in N_d (bottom right part of left panel).
- Almost all instance of **cloud breakup** (e.g., $LCC < 50\%$) occurs when **LWP is smaller than $60 g m^{-2}$** (right panel).
- Gray symbols: start (square), middle (star), and end (triangle) of simulations.
- The shades on small markers show RWP/LWP (left), and LCC (right).
- Dotted line: volume-mean droplet radius equal to $12 \mu m$ (critical radius)
- Dashed-dotted line: LWP equal to $60 g m^{-2}$



Cloud Morphology for 3 Select Runs



Evolution of Errors for 15 runs: Normalized bias = (LES - "Obs.") / "Obs."



5. Conclusions

- More than **2200 Lagrangian trajectories** are developed, and then meteorological, cloud, and aerosol variables from **reanalysis and satellite data are compiled** along each trajectory.
- Employing **PCA reduces the dimensionality** of the data needed to cover cloud field variability. PCA is useful in **efficiently selecting LES cases** that encompass the observed CCF phase space.
- Based on the PCA and phase space analysis, we identify more than **50 distinct cases representing a diverse array of environmental conditions**. These cases are used to **initiate 2-day detailed, high-resolution, large-domain LES experiments**.
- We employ SAM, which is coupled with a **prognostic aerosol scheme** that accounts for **aerosol budget tendencies** such as coalescence and interstitial scavenging, surface sources, and entrainment from the free troposphere.
- LES results for some cases demonstrate SAM's capability to **simulate observed conditions** and show the **sensitivity** of simulated cloud properties to **variations in environmental conditions**.
- The final LES simulations will enhance our understanding of **aerosol-cloud interactions** under a **spectrum of representative conditions**.

Acknowledgment

We acknowledge support from NOAA ERB through the MCB Project.

References

- Doelling, D. R., et al. (2016). Advances in geostationary-derived longwave fluxes for the CERES synoptic (SYN1deg) product. *J. Atmos. Oceanic Tech.*, 33 (3), 503–521.
- Eastman, R., Wood, R., & O, K-T. (2017). The subtropical stratocumulus-topped planetary boundary layer: A climatology and the Lagrangian evolution. *J. Atmos. Sci.*, 74, 2633–2656.
- Eastman, R., Lebock, M., & Wood, R. (2019). Warm Rain Rates from AMSR-E 89-GHz Brightness Temperatures Trained Using CloudSat Rain-Rate Observations. *J. Atmos. Oceanic Tech.*, 36(6), 1033–1051.
- Erfani, E., Blossey, P., Wood, R., Mohrman, J., Doherty, S., Wyant, M., & O, K. (2022). Simulating aerosol lifecycle impacts on the subtropical stratocumulus-to-cumulus transition using large-eddy simulations. *J. Geophys. Res.*, 127, e2022JD037258. <https://doi.org/10.1029/2022JD037258>
- Erfani, E., Wood, R., Blossey, P., Doherty, S., Eastman, R. (2024). Building a comprehensive library of observed Lagrangian trajectories for testing modeled cloud evolution, aerosol-cloud interactions, and marine cloud brightening. *EGU sphere [preprint submitted]*. <https://doi.org/10.5194/egusphere.2024.3237>
- Gelaro, R., et al. (2017). Modern-era retrospective analysis for research and applications, version 2 (MERRA-2). *J. Clim.*, 30(14), 5419–5454.
- Glassmeier, F., Hoffmann, F., Johnson, J. S., Yamaguchi, T., Carlaw, K. S., and Feingold, G. (2019). An emulator approach to stratocumulus susceptibility. *Atmos. Chem. Phys.*, 19, 10191–10203. <https://doi.org/10.5194/acp-19-10191-2019>.
- Hersbach, H., et al. (2020). The ERA5 global reanalysis. *Quart. J. Roy. Meteor. Soc.*, 146 (730), 1999–2049.
- Kawanishi, T., et al. (2003). The Advanced Microwave Scanning Radiometer for the Earth Observing System (AMSR-E), NASA's contribution to the EOS for global energy and water cycle studies. *IEEE Trans. Geosci. Remote. Sens.*, 41(2), 184–194.
- Wentz, F. J., et al. (2014). Remote Sensing Systems DMSPP SSM/I Daily Environmental Suite on 0.25 deg grid, Version 7. Remote Sensing Systems, Santa Rosa, CA.